**Title:**

Perceptual and non-perceptual dissimilarity measures for salt dome delineation

**Author(s):**

Muhammad Amir Shafiq* and Ghassan AlRegib

*Center for Energy and Geo Processing (CeGP),*

*School of Electrical and Computer Engineering,*

*Georgia Institute of Technology,*

*Atlanta, GA, 30332*

**amirshafiq@gatech.edu*

**Summary:**

In this paper, we propose and evaluate the performance of five different perceptual and non-perceptual dissimilarity measures, which are used to measure the texture dissimilarity between the two neighboring cubes that share a square face centered around the given voxel. The proposed measures are the building blocks of three dimensional Gradient of Texture (3D-GoT), which can quantify texture variations in three-dimensional space. The proposed dissimilarity measures exploit the strong coherence between neighboring seismic sections and compute cubes dissimilarity by incorporating all inline, crossline and time directions that make it effective as compared to those of 2D dissimilarity measures. The perceptual dissimilarity are consistent with human perception and yield better dissimilarity as compared to non-perceptual measures. The experimental results on the real dataset from the North Sea, F3 block illustrate that the perceptual dissimilarity measures are not only computationally more efficient but also yield better salt dome delineation results as compared to the non-perceptual dissimilarity measures.

## Introduction

The evaporation of water from the basin give rise to the depositions of the salt evaporites. These evaporites over long periods of time break through the sediment layers and form a diapir shaped structure called salt dome, which may span tens of kilometers in Earth's subsurface. The detection and delineation of salt domes is important as they form traps for petroleum and gas reservoirs because of their impermeability. Experienced interpreters can manually delineate the salt bodies by observing the texture and intensity variations within migrated seismic data. However, with the striking increase in the size of the seismic data in recent years, academia and industry have tilted toward semi-automated and intelligent computer models for salt domes delineation. Over the last few years, researchers have proposed several methods, which include edge-based detection methods by Aqrawi et al. (2011) and Amin and Deriche (2015b), texture-based methods by Berthelot et al. (2013), Shafiq et al. (2015b) and Wang et al. (2015), graph theory based methods by Shi and Malik (2000) and Felzenszwalb and Huttenlocher (2004) and different image processing techniques by Guillen et al. (2015), Amin and Deriche (2015a), Shafiq et al. (2015a) and Qi et al. (2015) to delineate different structures within seismic volume. The dissimilarity measures proposed by Hegazy et al. (2015) are limited to 2D seismic inlines and doesn't take into account the effects of texture coherence from the neighboring inlines. In this paper, we present one of the texture-based methods, three dimensional Gradient of Texture (3D-GoT) by Shafiq et al. (2015b), and demonstrate the role of perceptual and non-perceptual dissimilarity measures in its robustness and performance for salt domes delineation within migrated seismic volumes. The proposed 3D dissimilarity measures not only takes into account the crossline and time direction, but also considers the inline direction for dissimilarity calculation, which results in better performance as compared to the 2D dissimilarity measures.

## Theory

Given a 3D seismic data volume $\mathbf{V}$ of size $X \times Y \times T$, where $X$ represents crosslines, $Y$ represents inlines and $T$ represents time depth, we define the 3D-GoT, $G[x,y,t]$, as the perceptual dissimilarity of the texture between two neighboring cubes that share a square face centered around the given voxel $[x,y,t]$. The 3D-GoT is calculated along all three inline, crossline and time directions of volume $\mathbf{V}$. To evaluate the GoT in the x-direction (crossline), we calculate GoT at each voxel $[x,y,t]$ in x-direction. As we move the center point as shown in Fig. 1 and its two neighboring cubes, denoted $W_x$ and $W_{x+}$, in the x-direction along the blue line, the texture dissimilarity along the blue line using the function $d(\cdot)$, we yield the GoT profile as the curve shown at the bottom of Fig. 1. Theoretically, the highest dissimilarity, and hence the highest GoT value, is obtained when the center point falls exactly on the texture boundary. Similarly, GoT is also calculated along y and t directions. An adaptive global threshold is used to threshold the GoT map to yield a binary map, which is later used in region growing to form a 3D salt body. The 3D-GoT can perform robustly in the presence of noise and requires very few parameters as compared to other algorithms. The details of theory and processing framework of 3D-GoT can be found in Shafiq et al. (2015b), whereas a brief description to layout dissimilarity framework is given in this paper.

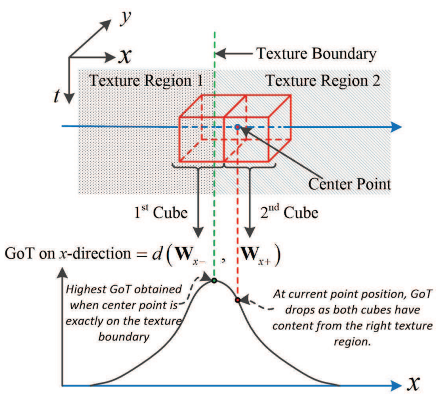


Figure 1: Illustration of GoT along x-direction

Table 1: The feature vector components

| Features | Intensity | Gradient |
|---|---|---|
| 1 | Mean | Mean |
| 2 | Std dev. | Std dev. |
| 3 | Skewness | Entropy |

The multi-scale 3D-GoT is mathematically expressed as

$$\mathbf{G}[x,y,t] = \left( \sum_{i\in\{x,y,t\}} \left( \sum_{n=1}^{N} \omega_n \cdot d\left(\mathbf{W}_{i-}^{n}, \mathbf{W}_{i+}^{n}\right)\right)^2 \right)^{\frac{1}{2}}, \tag{1}$$

$$\mathscr{F}[u,v,w] = \frac{1}{L^3} \sum_{x=0}^{L-1}\sum_{y=0}^{L-1}\sum_{t=0}^{L-1} f[x,y,t] e^{-2\pi i(xu+yv+tw)/L}, \tag{2}$$

where $\mathscr{F}\{\cdot\}$ represents the 3D-FFT, $\mathbf{W}_{-}^{n}$ and $\mathbf{W}_{+}^{n}$ represent the two cubes of size $n$ in negative and positive directions, respectively, with respect to the voxel at which GoT is calculated. $[x,y,t]$ and $[u,v,w]$ represent the coordinates of the spatial and frequency domains, respectively, and $L$ defines the edge length of a cube-shaped data volume. $d(\cdot)$ is dissimilarity function, which computes the perceptual dissimilarity between two cubes by applying two concatenated 3D-FFT magnitude operations to the absolute difference of neighboring cubes and averages the results using expectation operation $E$. The 3D-GoT measures the dissimilarity between the set of cubes along $x$, $y$ and $t$ directions. In this paper, we propose five different, three dimensional perceptual and non-perceptual texture dissimilarity measures for delineating salt domes within real seismic dataset. In the first, the dissimilarity measure is based on intensity and gradient statistics. We form the feature vectors, $\{\mathbf{F}_{-}, \mathbf{F}_{+}\} \in \mathbb{R}^6$ from the two neighboring cubes using intensity and gradient statistics summarized in Table 1, and then compute dissimilarity using the 2-norm of the difference between the feature vectors as

$$d_1(\mathbf{W}_{i-}, \mathbf{W}_{i+}) = \|\mathbf{F}_{i-} - \mathbf{F}_{i+}\|, \quad i \in \{x,y,t\}. \tag{3}$$

The second measure is based on singular values in which we compute the dissimilarity using the 2-norm of the difference between the feature vectors $\mathbf{F}_{-}$ and $\mathbf{F}_{+}$ formed by arranging the three dimensional singular value decomposition in descending order as

$$d_2(\mathbf{W}_{i-}, \mathbf{W}_{i+}) = \|\mathbf{F}_{i-} - \mathbf{F}_{i+}\|, \quad i \in \{x,y,t\}. \tag{4}$$

In the third dissimilarity measure based on Fourier coefficients, we compute the 3D-FFT of the neighboring cubes along x, y and t directions, and measure dissimilarity as the mean of absolute difference between the magnitude spectra of the two cubes. Mathematically,

$$d_3(\mathbf{W}_{i-}, \mathbf{W}_{i+}) = E(|\,|\mathscr{F}\{\mathbf{W}_{i-}\}| - |\mathscr{F}\{\mathbf{W}_{i+}\}|\,|), \quad i \in \{x,y,t\}. \tag{5}$$

The fourth dissimilarity measure is based on error spectrum chaos that measures the disorder or irregularity of texture inside the neighboring cubes in the absolute error sense. Hegazy et al. (2015) showed that this measure is consistent with human perception, and is also computationally less expensive. Mathematically,

$$E_{Mag} = E(|\mathscr{F}\{|\mathscr{F}\{\nabla\{|\mathbf{W}_{i-} - \mathbf{W}_{i+}|\}\}|\}|), \tag{6}$$

$$E_{Ph} = E(|\mathscr{F}\{\angle\mathscr{F}\{|\mathbf{W}_{i-} - \mathbf{W}_{i+}|\}\}|), \tag{7}$$

$$d_4(\mathbf{W}_{i-}, \mathbf{W}_{i+}) = E_{Mag} + \alpha E_{Ph}, \quad i \in \{x,y,t\}, \tag{8}$$

where $E(\cdot)$ is the expectation operator, $\nabla$ is the gradient operator and $\alpha$ is an empirically selected weighing factor for phase spectrum. The fifth dissimilarity measure is based on the error magnitude spectrum chaos, similar to $d_4(\cdot)$, however phase information is dropped ($\alpha = 0$) because only intensity contains information about statistical measures. Mathematically,

$$d_5(\mathbf{W}_{i-}, \mathbf{W}_{i+}) = E(|\mathscr{F}\{|\mathscr{F}\{|\mathbf{W}_{i-} - \mathbf{W}_{i+}|\}|\}|), \quad i \in \{x,y,t\}. \tag{9}$$

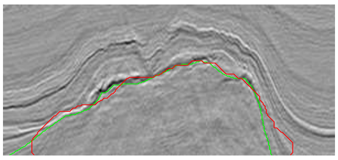

(a) $d_1(\cdot)$

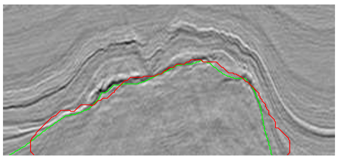

(b) $d_2(\cdot)$

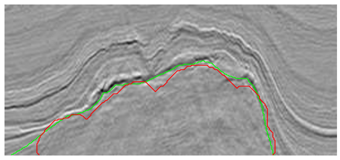

(c) $d_3(\cdot)$

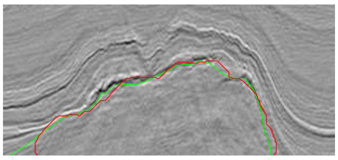

(d) $d_4(\cdot)$

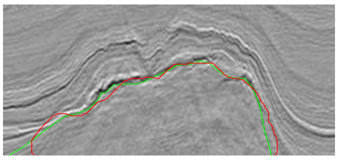

(e) $d_5(\cdot)$

Figure 2: Experimental results of 3D-GoT on section section inline #389 with different dissimilarity functions $d(\cdot)$. Green: Ground Truth, Red: 3D-GoT by Shafiq et al. (2015b).

## Experimental Results

In this section, we evaluate the effect of different dissimilarity measures on 3D-GoT performance. We have used the real seismic dataset acquired from the Netherlands offshore, F3 block in the North Sea by dGB Earth Sciences (1987). The seismic volume that contains the salt dome structure has an inline number ranging from #151 to #501, a crossline number ranging from #401 to #701, and a time direction ranging from 1,300ms to 1,848ms sampled every 4ms. The results of salt dome delineation using different dissimilarity measures for seismic section inline #389 are shown in Fig. 2. The output of 3D-GoT is labelled in red color, whereas the ground truth is manually labeled in green. The subjective assessment show that all dissimilarity measures yield good results, however, the boundaries detected by perceptual dissimilarity measures, $d_4(\cdot)$ and $d_5(\cdot)$, are more closer to the ground truth as compared to those detected by non-perceptual dissimilarity measures. To objectively evaluate the similarity between the detected boundaries and the ground truth, we have used the Fréchet distance based similarity index, *SalSIM* by Wang et al. (2015). The *SalSIM* index varies between 0 and 1, indicating minimum and maximum similarity between the two curves, respectively. The *SalSIM* indices of the twenty consecutive seismic section inlines with different dissimilarity measures along with their mean and standard deviation are shown in Table. 2. The mean and standard deviation of *SalSIM* indices show that the best and second best results are obtained using $d_5(\cdot)$ and $d_4(\cdot)$, respectively that are in accordance with subjective evaluation. The time complexity is also summarized in Table. 2, which show $d_5(\cdot)$ is computationally more efficient as compared to other dissimilarity measures.

## Conclusions

In this paper, we have proposed five different, three dimensional perceptual and non-perceptual texture dissimilarity measures for 3D-GoT as an extension of previous work on two dimensional dissimilarity measures. We have also evaluated the performance of different dissimilarity measures for salt dome delineation. The experimental results on the real dataset from the North Sea, F3 block demonstrate that perceptual dissimilarity measures, which are consistent with human perception, performs better and are also computationally more efficient as compared to non-perceptual dissimilarity measures.

## Acknowledgements

This work is supported by the Center for Energy and Geo Processing (CeGP) at the Georgia Institute of Technology and King Fahd University of Petroleum and Minerals.

Table 2: SalSIM indices of 3D-GoT with different dissimilarity measures

| Seismic Sections | $d_1(\mathbf{W}_{i-},\mathbf{W}_{i+})$ | $d_2(\mathbf{W}_{i-},\mathbf{W}_{i+})$ | $d_3(\mathbf{W}_{i-},\mathbf{W}_{i+})$ | $d_4(\mathbf{W}_{i-},\mathbf{W}_{i+})$ | $d_5(\mathbf{W}_{i-},\mathbf{W}_{i+})$ |
|---|---|---|---|---|---|
| #389 | 0.9037 | 0.9091 | 0.9077 | 0.9160 | 0.9248 |
| #390 | 0.8695 | 0.9040 | 0.9075 | 0.9153 | 0.9328 |
| #391 | 0.7147 | 0.8750 | 0.9127 | 0.9077 | 0.9239 |
| #392 | 0.8755 | 0.8997 | 0.9030 | 0.9101 | 0.9166 |
| #393 | 0.8429 | 0.8953 | 0.9189 | 0.9073 | 0.9250 |
| #394 | 0.8694 | 0.8987 | 0.9041 | 0.9157 | 0.9320 |
| #395 | 0.7057 | 0.8725 | 0.8986 | 0.9079 | 0.9095 |
| #396 | 0.8306 | 0.8934 | 0.9060 | 0.9179 | 0.9273 |
| #397 | 0.9235 | 0.8984 | 0.9009 | 0.9071 | 0.9096 |
| #398 | 0.8994 | 0.8980 | 0.8928 | 0.9024 | 0.9038 |
| #399 | 0.9241 | 0.9092 | 0.8852 | 0.9124 | 0.9132 |
| #400 | 0.9195 | 0.9004 | 0.9061 | 0.9094 | 0.9143 |
| #401 | 0.8852 | 0.9182 | 0.9143 | 0.9241 | 0.9258 |
| #402 | 0.9154 | 0.9121 | 0.9048 | 0.9134 | 0.9145 |
| #403 | 0.9295 | 0.9241 | 0.9002 | 0.9129 | 0.9337 |
| #404 | 0.8906 | 0.9290 | 0.9037 | 0.9165 | 0.9370 |
| #405 | 0.9303 | 0.9470 | 0.8766 | 0.9347 | 0.9420 |
| #406 | 0.9484 | 0.9444 | 0.8975 | 0.9279 | 0.9429 |
| #407 | 0.9250 | 0.9424 | 0.8872 | 0.9297 | 0.9419 |
| #408 | 0.9321 | 0.9229 | 0.8397 | 0.9208 | 0.9331 |
| #409 | 0.9357 | 0.9398 | 0.8674 | 0.9068 | 0.9277 |
| **Mean** | 0.8843 | 0.9111 | 0.8969 | 0.9150 | 0.9253 |
| **Std. Dev.** | 0.0658 | 0.0213 | 0.0180 | 0.0084 | 0.0115 |
| **Time (s)** | 139.0591 | 12.9008 | 12.1924 | 38.8589 | 12.0147 |

## References

Amin, A. and Deriche, M. [2015a] A hybrid approach for salt dome detection in 2D and 3D seismic data. In: *Image Processing (ICIP), 2015 IEEE International Conference on*. 2537–2541.

Amin, A. and Deriche, M. [2015b] A new approach for salt dome detection using a 3D multidirectional edge detector. *Applied Geophysics*, **12**(3), 334–342.

Aqrawi, A.A., Boe, T.H. and Barros, S. [2011] Detecting salt domes using a dip guided 3D Sobel seismic attribute. In: *Expanded Abstracts of the SEG 81st Annual Meeting*. Society of Exploration Geophysicists, 1014–1018.

Berthelot, A., Solberg, A.H. and Gelius, L.J. [2013] Texture attributes for detection of salt. *Journal of Applied Geophysics*, **88**, 52–69.

dGB Earth Sciences, B. [1987] The Netherlands Offshore, The North Sea, F3 Block - Complete. *https://opendtect.org/osr/pmwiki.php/Main/Netherlands/OffshoreF3BlockComplete4GB*.

Felzenszwalb, P.F. and Huttenlocher, D.P. [2004] Efficient graph-based image segmentation. *International Journal of Computer Vision*, **59**(2), 167–181.

Guillen, P., Larrazabal, G., Gonzalez, G., Boumber, D. and Vilalta, R. [2015] *Supervised learning to detect salt body*, chap. 351. 1826–1829.

Hegazy, T., Wang, Z. and AlRegib, G. [2015] The Role of Perceptual Texture Dissimilarity in Automating Seismic Data Interpretation. *Proc. IEEE Global Conf. on Signal and Information Processing (GlobalSIP), Orlando, Florida, Dec. 14-16*.

Qi, J., Cahoj, M., AlAli, A., Li, L. and Marfurt, K. [2015] *Segmentation of salt domes, mass transport complexes on 3D seismic data volumes using Kuwahara windows and multiattribute cluster analysis*, chap. 350. 1821–1825.

Shafiq, M.A., Wang, Z. and Alregib, G. [2015a] Seismic interpretation of migrated data Using edge-based geodesic active contours. In: *Proc. IEEE Global Conf. on Signal and Information Processing (GlobalSIP), Orlando, Florida, Dec. 14-16*.

Shafiq, M.A., Wang, Z., Amin, A., Hegazy, T., Deriche, M. and AlRegib, G. [2015b] Detection of Salt-dome Boundary Surfaces in Migrated Seismic Volumes Using Gradient of Textures. In: *Expanded Abstracts of the SEG 85th Annual Meeting, New Orleans, Louisiana*. 1811–1815.

Shi, J. and Malik, J. [2000] Normalized cuts and image segmentation. *Pattern Analysis and Machine Intelligence, IEEE Transactions on*, **22**(8), 888–905.

Wang, Z., Hegazy, T., Long, Z. and AlRegib, G. [2015] Noise-robust detection and tracking of salt domes in postmigrated volumes using texture, tensors, and subspace learning. *Geophysics*, **80**(6).